AIMS Mathematics, 10(5): 11071–11085.
DOI: 10.3934/math.2025502
Received: 21 March 2025
Revised: 27 April 2025
Accepted: 08 May 2025
Published: 15 May 2025

https://www.aimspress.com/journal/Math

Research article

The powerful closed form technique for the modified equal width equation with numerical simulation

Abdulhamed Alsisi*

Department of Mathematics, College of Science, Taibah University, Al-Madinah Al-Munawarah, Saudi Arabia

* **Correspondence:** Email: ahsisi@taibahu.edu.sa.

Abstract: This work introduces the closed form approach to generate solitary wave solutions to the modified equal width (MEW) model. This model generalizes the equal width (EW) equation, which characterizes wave propagation in shallow water. It aims to better represent nonlinear and dispersive effects by altering the original model's terms. Because of its simplicity, reliability, and efficiency, the proposed technique has the potential to be applied to a range of nonlinear partial differential equations (NPDEs) in practical research. We also employ the finite difference method to provide the numerical solution for the MEW model. A comparison with the analytical solution we arrived at demonstrates the method's accuracy. This work shows that the numerical method stays stable and accurate despite alterations in time stepping, wave speed, and spatial discretization. This also allows further exploration of nonlinear models that accurately depict significant physical processes in our everyday existence.

Keywords: closed form approach; soliton solutions; MEW model; extended tanh method; numerical methods; fluid dynamics
Mathematics Subject Classification: 76B25, 35C05, 35C07, 35Q35, 35Q53, 65M20

1. Introduction

Nonlinear partial differential equations (NPDEs) are widely used in scientific areas, such plasma physics, biological sciences, chemical engineering, chemical processes, optical fibers, superfluids, etc., for describing complex phenomena [1, 2] and references therein. The analytical and numerical solutions of these equations, particularly, the soliton solutions, which have recently become among the most noteworthy topics for mathematicians and physicists, are necessary to comprehend these physical processes, see for example [3, 4]. Nonlinear waves refer to wave phenomena in which the principle of superposition is not applicable, owing to the nonlinear characteristics of the governing

equations [5, 6]. Nonlinear wave theory is essential for understanding real-world phenomena in fluids, plasmas, mechanical systems, optics, and biological systems. Many recent studies have examined the behavior of nonlinear waves using different models of NPDEs [7, 8].

One may define a solitary wave as a wave whose form and size, while observed in the context of traveling at the wave's group velocity, is independent of any temporal development [9]. Solitary waves can arise from a variety of events, such as increasing light intensity in optical cables or rising water surfaces. Due to the intricate nature and challenges associated with achieving a multi-wavelength soliton state, there is a limited amount of information available regarding its internal dynamic characteristics [10]. The mathematical justification of these particular events yields the NPDEs [11, 12]. Understanding these physical processes more effectively is potentially possible by looking at the analytical solutions to different NPDEs. The water wave soliton arises from the wave's propensity to disperse, a dynamic balance between nonlinear effects and dispersion. There are other applications for soliton waves in the field of applied science [13–15].

Wave propagation in dispersive and nonlinear media is described by the modified equal width (MEW) equation, a nonlinear partial differential equation (NPDE) [16]. It is an expansion of the equal width (EW) equation with changes made to better account for physical phenomena such nonlinear dispersion, wave steepening, and soliton interactions. Fluid dynamics, ion acoustic plasma waves, plasma physics, and other applied disciplines frequently employ the MEW equation [17], showing the importance of this equation. The equation produces an undular bore of the same breadth [18]. This model is really connected with the modified regularized long wave model and the modified Korteweg-de Vries equation [19]. Wazwaz applied the tanh and sine-cosine approaches to investigate the MEW equation and two of its modifications [20]. Saka and Dağ examined a solution based on a collocation approach that incorporates cubic B-splines [21]. Başhan et al. used the the fifth-order quintic B-spline-based scheme and a forward finite difference formula for finding approximate solutions to the MEW equation [22]. Yağmurlu and Karakaş numerically solved the MEW equation utilizing an innovative approach that employs the collocation finite element method, incorporating trigonometric cubic B-splines as the approximating functions [23]. Fan and Wu applied the fourth-order improvised cubic B-spline collocation method to numerically solve the MEW equation [24]. Kirli and Cikit developed a high-order accurate hybrid technique to construct an approximate solution of the MEW equation [25]. The MEW equation has a few analytical solutions, along with certain beginning and boundary conditions. As a result, comparing the MEW equation's analytical and numerical solutions will be an interesting task. The MEW model is presented as follows [16, 19, 26]:

$$\chi_t + 3\chi^2\chi_x - \mu\chi_{xxt} = 0, \tag{1.1}$$

where μ is a constant, and $\chi(x, t)$ denotes the wave profile. This equation is a nonlinear wave equation with cubic nonlinearity and a pulse-like solitary wave solution. It is essential to comprehend and investigate these equations in order to accurately simulate physical processes and elucidate nonlinear wave dynamics in dispersive media.

We apply the closed-form approach to solve the MEW model. Using unrestricted physical parameters, this technique gives several families of solitary wave solutions. It also provides us with important solitary wave responses and saves us from tiresome and complicated computations, among other advantages. This strategy is well-designed. This technique might be beneficial for mathematicians, engineers, and physicists as a box solver. The numerical solution for the MEW model

is illustrated using a powerful finite difference approach. The accuracy of this approach is shown by a comparison with the presented analytical solution. This study demonstrates that changes in time stepping, wave speed, and spatial discretization do not affect the numerical method's stability and accuracy. Our findings demonstrate the effectiveness of the suggested technique and how it may be utilized to solve a wide variety of applied science and creative physics models.

The structure of this work is as follows. Section 2 explains the expanded tanh technique. Section 3 includes closed-form solutions for the MEW model. Section 4 shows graphical representations of selected solutions to illustrate their behavior. We also explore the interpretation of the data to evaluate the success of the proposed technique. Section 5 provides a numerical investigation of the MEW model and a comparison with the exact solutions. Lastly, we provide some closing thoughts on our findings in Section 6.

2. The description of the technique

This section provides a simplified version of the extended tanh technique [27, 28]. Assume that the NPDEs for $\chi(x,t)$ have the following form:

$$\mathfrak{G}(\chi,\chi_t,\chi_x,\chi_{tt},\chi_{xt},\chi_{xx},....) = 0, \tag{2.1}$$

where $\chi = \chi(x,t)$ denotes an unknown function. We utilize the wave transformation

$$\zeta = x + vt, \tag{2.2}$$

where v is the wave speed. Putting Eq (2.2) into Eq (2.1) changes it into an ODE

$$\mathfrak{H}(\chi,\chi',\chi'',\chi''',.....) = 0. \tag{2.3}$$

Step 1. The solution of Eq (2.3) is given as

$$\chi(\zeta) = a_0 + \sum_{j=0}^{l=N} a_l\phi^l(\xi) + b_l\phi^{-l}(\zeta). \tag{2.4}$$

There are constants to be found, namely $a_k(j = 0, 1, ..., N)$, and the function $\phi(\zeta)$ satisfies the Riccati equation provided by

$$\phi' = \varpi + \phi^2(\zeta), \tag{2.5}$$

where ϖ is a constant to be determined. Eq (2.5)'s validated solutions are as follows.

1. If $\varpi < 0$, then

$$\begin{aligned} \phi(\zeta) &= -\sqrt{-\varpi}\, tanh(\sqrt{-\varpi}\,\zeta), \\ \phi(\zeta) &= -\sqrt{-\varpi}\, coth(\sqrt{-\varpi}\,\zeta). \end{aligned} \tag{2.6}$$

2. If $\varpi > 0$, then

$$\begin{aligned} \phi(\zeta) &= \sqrt{\varpi}\, tan(\sqrt{\varpi}\,\zeta), \\ \phi(\zeta) &= -\sqrt{\varpi}\, cot(\sqrt{\varpi}\,\zeta). \end{aligned} \tag{2.7}$$

3. If $\varpi = 0$, then

$$\phi(\xi) = -\frac{1}{\zeta}. \tag{2.8}$$

Step 2. Balancing the highest power nonlinear term in (2.3) with the highest-order derivative term provides N.

Step 3. Substituting Eqs (2.4) and (2.5) into Eq (2.3) yields a set of nonlinear algebraic equations with zero coefficients for each power of $\phi(\zeta)$. Solving these equations yields the expression of Eq (2.4). Thus, using Eqs (3.12), (2.7), and (3.26) gives the desired explicit solutions of Eq (2.1).

3. Solutions of the MEW equation

Here, we use the wave transformation

$$\chi(x,t) = \chi(\zeta), \quad \zeta = x - v\,t, \tag{3.1}$$

where w denotes the wave speed. Eq (3.1) is substituted into Eq (1.1) to produce

$$\eta_1 \chi'' + \eta_2 \chi^3 + \eta_3 \chi = 0, \tag{3.2}$$

$\eta_1 = \mu\, v$, $\eta_2 = 1$, $\eta_3 = -v$. Balancing the highest-order derivatives with nonlinear terms gives $N = 1$. Thus

$$\chi(\zeta) = a_0 + a_1\phi + \frac{b_1}{\phi}, \tag{3.3}$$

$$\chi'(\zeta) = a_1\varpi + a_1\phi^2 - \frac{b_1\varpi}{\phi^2} - b_1. \tag{3.4}$$

Substituting Eq (3.3) and its derivative into Eq (3.2) and collecting all terms with the same power of ϕ^3, ϕ^2, ϕ, ϕ^0, ϕ^{-1}, ϕ^{-2}, and ϕ^{-3} gives

$$2\eta_1 a_1 + a_1^3\eta_2 = 0, \tag{3.5}$$

$$3a_0a_1^2\eta_2 = 0, \tag{3.6}$$

$$3a_0^2a_1\eta_2 + 3a_1^2\eta_2 b_1 + a_1\eta_3 + 2\eta_1 a_1\varpi = 0, \tag{3.7}$$

$$a_0^3\eta_2 + 6a_0a_1\eta_2 b_1 + a_0\eta_3 = 0, \tag{3.8}$$

$$3a_0^2\eta_2 b_1 + 3a_1\eta_2 b_1^2 + b_1\eta_3 + 2\eta_1 b_1\varpi = 0, \tag{3.9}$$

$$3a_0\eta_2 b_1^2 = 0, \tag{3.10}$$

$$\eta_2 b_1^3 + 2\eta_1 b_1\varpi^2 = 0. \tag{3.11}$$

Solving these equations, gives the following cases.

Case 1.

$$a_0 = 0, \quad a_1 = \pm\sqrt{\frac{-2\eta_1}{\eta_2}},\ b_1 = 0, \varpi = -\frac{\eta_3}{2\eta_1}. \tag{3.12}$$

Putting Eq (3.12) into Eq (3.3), we get the following solutions.

For $\frac{\eta_3}{\eta_1} > 0$, the solutions of (3.2) are

$$\chi_{1,2}(\zeta) = \pm \sqrt{\frac{-\eta_3}{\eta_2}}\, tanh(\sqrt{\frac{\eta_3}{2\eta_1}}\,\zeta), \tag{3.13}$$

$$\chi_{3,4}(\zeta) = \pm \sqrt{\frac{-\eta_3}{\eta_2}}\, coth(\sqrt{\frac{\eta_3}{2\eta_1}}\,\zeta). \tag{3.14}$$

Thus, the solutions of (1.1) are

$$\chi_{1,2}(x,t) = \pm \sqrt{\frac{-\eta_3}{\eta_2}}\, tanh(\sqrt{\frac{\eta_3}{2\eta_1}}\,(x - v\,t)), \tag{3.15}$$

$$\chi_{3,4}(x,t) = \pm \sqrt{\frac{-\eta_3}{\eta_2}}\, coth(\sqrt{\frac{\eta_3}{2\eta_1}}\,(x - v\,t)). \tag{3.16}$$

For $\frac{\eta_3}{\eta_1} < 0$, the solutions of (3.2) are

$$\begin{aligned} \chi_{5,6}(\zeta) &= \pm \sqrt{\frac{\eta_3}{\eta_2}}\, tan(\sqrt{\frac{-\eta_3}{2\eta_1}}\,\zeta), \\ \chi_{7,8}(\zeta) &= \mp \sqrt{\frac{\eta_3}{\eta_2}}\, cot(\sqrt{\frac{-\eta_3}{2\eta_1}}\,\zeta). \end{aligned} \tag{3.17}$$

Thus the solutions of (1.1) are

$$\begin{aligned} \chi_{5,6}(x,t) &= \pm \sqrt{\frac{\eta_3}{\eta_2}}\, tan(\sqrt{\frac{-\eta_3}{2\eta_1}}\,(x - v\,t)), \\ \chi_{7,8}(x,t) &= \mp \sqrt{\frac{\eta_3}{\eta_2}}\, cot(\sqrt{\frac{-\eta_3}{2\eta_1}}\,(x - v\,t)). \end{aligned} \tag{3.18}$$

For $\frac{\eta_3}{\eta_1} = 0$, the solutions of (3.2) are

$$\chi_{9,10}(\zeta) = \pm \sqrt{\frac{-2\eta_1}{\eta_2}}\frac{-1}{\zeta}. \tag{3.19}$$

Thus the solutions of (1.1) are

$$\chi_{9,10}(x,t) = \pm \sqrt{\frac{-2\eta_1}{\eta_2}}\,\frac{1}{x - v\,t}. \tag{3.20}$$

Case 2.

$$a_0 = 0, \quad a_1 = \pm \sqrt{\frac{-2\eta_1}{\eta_2}},\ b_1 = \mp \frac{\eta_3}{2\sqrt{2}\sqrt{-\eta_1\eta_2}}, \varpi = \frac{\eta_3}{4\eta_1}. \tag{3.21}$$

For $\frac{\eta_3}{\eta_1} < 0$, the solutions of (3.2) are

$$\chi_{11,12}(\zeta) = \pm \sqrt{\frac{\eta_3}{2\eta_2}}\left(tanh\left(\sqrt{\frac{-\eta_3}{4\eta_1}}\,\zeta\right) - coth\left(\sqrt{-\frac{\eta_3}{4\eta_1}}\,\zeta\right)\right). \tag{3.22}$$

Thus the solutions of (1.1) are

$$\chi_{11,12}(x,t) = \pm\sqrt{\frac{\eta_3}{2\eta_2}}\left(tanh\left(\sqrt{\frac{-\eta_3}{4\eta_1}}\,(x-v\,t)\right) - \,coth\left(\sqrt{-\frac{\eta_3}{4\eta_1}}\,(x-v\,t)\right)\right). \tag{3.23}$$

For $\frac{\eta_3}{\eta_1} > 0$, the solutions of (3.2) are

$$\chi_{13,14}(\zeta) = \pm\sqrt{\frac{-\eta_3}{2\eta_2}}\left(tan\left(\sqrt{\frac{\eta_3}{4\eta_1}}\,\zeta\right) + \,cot\left(\sqrt{\frac{\eta_3}{4\eta_1}}\,\zeta\right)\right). \tag{3.24}$$

Thus the solutions of (1.1) are

$$\chi_{13,14}(x,t) = \pm\sqrt{\frac{-\eta_3}{2\eta_2}}\left(tan\left(\sqrt{\frac{\eta_3}{4\eta_1}}\,(x-v\,t)\right) + \,cot\left(\sqrt{\frac{\eta_3}{4\eta_1}}\,(x-v\,t)\right)\right). \tag{3.25}$$

For $\frac{\eta_3}{\eta_1} = 0$, the solutions of (1.1) are identical to the solutions provided in (3.20).

Case 3.

$$a_0 = 0, \quad a_1 = \pm\sqrt{\frac{-2\eta_1}{\eta_2}}, \; b_1 = \mp\frac{\eta_3}{4\sqrt{2}\sqrt{-\eta_1\eta_2}}, \varpi = -\frac{\eta_3}{8\eta_1}. \tag{3.26}$$

For $\frac{\eta_3}{\eta_1} < 0$, the solutions of (3.2) are

$$\chi_{15,16}(\zeta) = \pm\sqrt{\frac{\eta_3}{4\eta_2}}\left(tan\left(\sqrt{-\frac{\eta_3}{8\eta_1}}\,\zeta\right) - \,cot\left(\sqrt{-\frac{\eta_3}{8\eta_1}}\,\zeta\right)\right). \tag{3.27}$$

Thus the solutions of (1.1) are

$$\chi_{15,16}(x,t) = \pm\sqrt{\frac{\eta_3}{4\eta_2}}\left(tan\left(\sqrt{-\frac{\eta_3}{8\eta_1}}\,(x-v\,t)\right) - \,\sqrt{\frac{\eta_3}{4\eta_2}}\,cot\left(\sqrt{-\frac{\eta_3}{8\eta_1}}\,(x-v\,t)\right)\right). \tag{3.28}$$

For $\frac{\eta_3}{\eta_1} > 0$, the solutions of (3.2) are

$$\chi_{17,18}(\zeta) = \pm\sqrt{-\frac{\eta_3}{4\eta_2}}\left(tanh\left(\sqrt{\frac{\eta_3}{8\eta_1}}\,\zeta\right) + coth\left(\sqrt{\frac{\eta_3}{8\eta_1}}\,\zeta\right)\right). \tag{3.29}$$

Thus the solutions of (1.1) are

$$\chi_{17,18}(x,t) = \pm\sqrt{-\frac{\eta_3}{4\eta_2}}\left(tanh\left(\sqrt{\frac{\eta_3}{8\eta_1}}\,(x-v\,t)\right) + coth\left(\sqrt{\frac{\eta_3}{8\eta_1}}\,(x-v\,t)\right)\right). \tag{3.30}$$

For $\frac{\eta_3}{\eta_1} = 0$, the solutions of (1.1) are identical to the solutions provided in (3.20).

4. Graphical representation

In this part, the solutions obtained by applying the closed-form method to the MEW are visually demonstrated using MATLAB. We illustrate the solutions that we provided with several two- and three-dimensional examples. The physical characteristics of the acquired solution (3.15) are shown in Figures 1 and 2, where $x \in [-10, 10]$, $t \in [0, 1]$, $v = 4$, and $\mu = -1$. Namely, Figure 1

represents the three-dimensional (3D) kink wave for the corresponding solution. Figures 2 shows the two-dimensional (2D) localized soliton wave solution. Figure 3(a) represents 2D kink wave solution in (3.15), where $x \in [-1, 5]$, $v = 4$, and $\mu = -0.01$, but taking different snapshots by varying $t = \{0, 0.2, 0.4, 0.6, 0.8, 1\}$, to exhibit the influence of time on the solution, displaying a soliton wave's transition with time. Similarly, Figure 3(b) shows the effects of varying $\mu = \{-0.001, -0.01, -0.1, -0.5, -1, -2, -3, -4, -5\}$ on the same solution with $x \in [-3, 3]$, $t = 0$, and $v = 4$. Figure 4(a) shows 2D solitary wave solution given in Eq (3.18), where $x \in [-0.985, -0.97]$, $t = 0$, $v = -4$, and $\mu = 1$. Figure 4(b) shows the 2D solitary wave solution given in Eq (3.23), where $x \in [-0.2, 0.2]$, $t = 0$, $v = -4$, and $\mu = 1$.

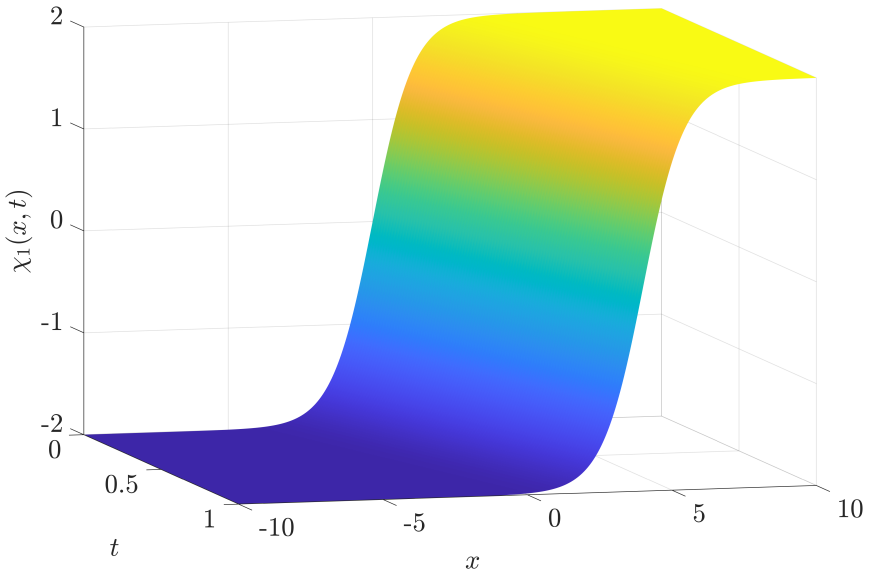

Figure 1. A 3D plot of the solution $\chi_1(x, t)$ given in Eq (3.15), with $x \in [-10, 10]$, $t \in [0, 1]$, wave velocity $v = 4$, and $\mu = -1$.

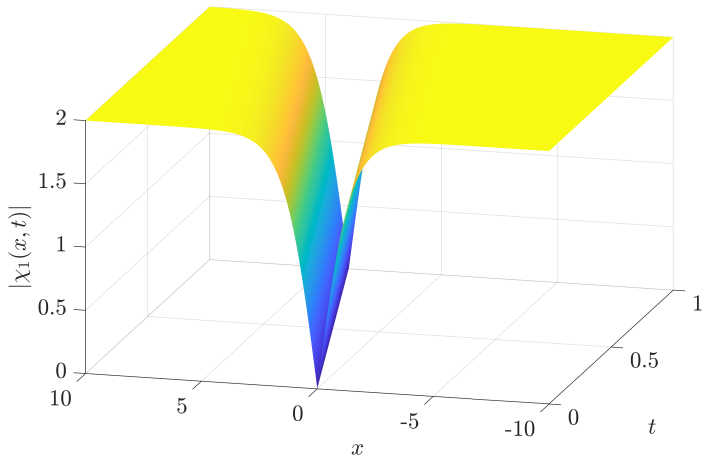

Figure 2. A 3D plot of the absolute value of the solution $|\chi_1(x, t)|$ given in (3.15) for $x \in [-10, 10]$, $t \in [0, 1]$, with parameters $v = 4$, and $\mu = -1$.

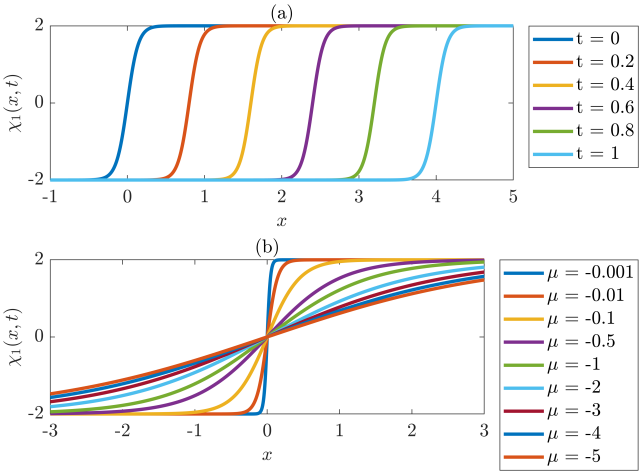

Figure 3. (a) Evolution over time ($t \in \{0, 0.2, \ldots, 1\}$) of the solution $\chi_1(x,t)$ given in (3.15) for $x \in [-1, 5]$, with the parameters $v = 4$ and $\mu = -0.01$. (b) This figure shows the solution $\chi_1(x,t)$ given in (3.15) depending on μ ($\mu \in \{-0.001, -0.01, \ldots, -5\}$) at $t = 0$, with $x \in [-3, 3]$ and $v = 4$.

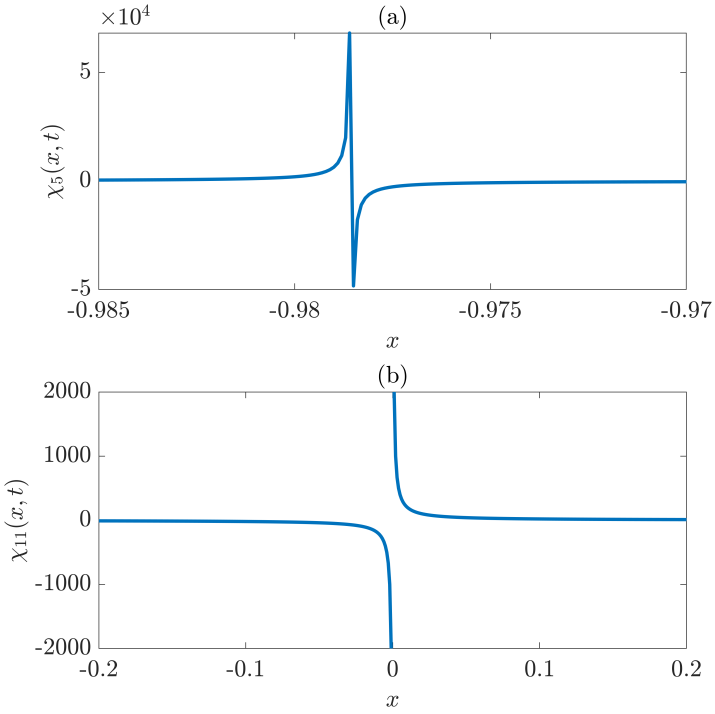

Figure 4. (a) 2D plot of the solution $\chi_5(x,t)$ given in (3.18) at $t = 0$ and $x \in [-0.985, -0.97]$, with the parameters $v = -4$, and $\mu = 1$. (b) 2D plot of the solution $\chi_{11}(x,t)$ given in (3.23) at $t = 0$ and $x \in [-0.2, 0.2]$, with the parameters $v = -4$ and $\mu = 1$.

5. Numerical method and test cases

The numerical approach employed here is described in this section, along with a comparison of the results with previously obtained analytical solutions [29]. First, we construct a discrete function that

approximates the solution given in (1.1), i.e., $\tilde{\chi}_{i,j} \approx \chi(x,t)$. A uniform partition is made both spatially and temporally, such as $x_i = x_0 + ih$, $i = 0, 1, .., M$, $h = (x_M - x_0)/M$, and $t_j = j\delta t$ for $j = 0, 1, .., N$, where $\delta t = T/N$ for $t \in [0, T]$. First, we need to rewrite Eq (1.1) in conservative form as follows:

$$\chi_t + (\chi^3)_x - \mu\chi_{xxt} = 0. \tag{5.1}$$

By approximating the time derivative with forward difference and the spatial first derivative with Crank–Nicolson approximation and central difference approximation for the second derivative, we get the following explicit numerical scheme:

$$\begin{aligned} &\frac{\tilde{\chi}_{i,j+1} - \tilde{\chi}_{i,j}}{\delta t} + \frac{1}{4h}\left(\tilde{\chi}^3_{i+1,j+1} - \tilde{\chi}^3_{i-1,j+1} + \tilde{\chi}^3_{i+1,j} - \tilde{\chi}^3_{i-1,j}\right) \\ &- \frac{\mu}{\delta t(h)^2}\left(\tilde{\chi}_{i+1,j+1} - 2\tilde{\chi}_{i,j+1} + \tilde{\chi}_{i-1,j+1} - \tilde{\chi}_{i+1,j} + 2\tilde{\chi}_{i,j} - \tilde{\chi}_{i-1,j}\right) = 0. \end{aligned} \tag{5.2}$$

Using Taylor expansion for $\tilde{\chi}^3_{i,j+1}$, i.e, $\tilde{\chi}^3_{i,j+1} = \tilde{\chi}^3_{i,j} + \delta t\frac{\partial\tilde{\chi}^3_{i,j}}{\partial t}$, to simplify the nonlinear system of equations in Eq (5.2) and approximating the time derivatives using finite difference techniques produces $\tilde{\chi}^3_{i,j+1} \approx \tilde{\chi}^3_{i,j} + 3\tilde{\chi}^2_{i,j}(\tilde{\chi}_{i,j+1} - \tilde{\chi}_{i,j})$. Then Eq (5.2) is reformed into the following system of linear equations for z_i by allowing $z_i = \tilde{\chi}_{i,j+1} - \tilde{\chi}_{i,j}$, and $r = \frac{3}{4h}$:

$$\alpha_1 z_i + \alpha_2 z_{i+1} - \alpha_3 z_{i-1} = 2r(\tilde{\chi}^3_{i-1,j} - \tilde{\chi}^3_{i+1,j}), \tag{5.3}$$

where

$$\begin{aligned} \alpha_1 &= \frac{1}{\delta t} + \frac{2\mu}{\delta t\, h^2}, \\ \alpha_2 &= r\tilde{\chi}^2_{i+1,j} - \frac{\mu}{\delta t\, h^2}, \\ \alpha_3 &= r\tilde{\chi}^2_{i-1,j} + \frac{\mu}{\delta t\, h^2}. \end{aligned}$$

As a result, the right-hand side of Eq (5.3) becomes known, leading to a linear system. We then compute z_i and update the next iteration using $\tilde{\chi}_{i,j+1} = \tilde{\chi}_{i,j} + z_i$. Next, we apply the numerical approach described in this section to various test problems. Furthermore, the definition of the $L2$-norm used here is the following:

$$\|\chi - \tilde{\chi}\|_2 = \sqrt{\sum_{i=1}^{n} \frac{|\chi_i - \tilde{\chi}|^2}{M}},$$

where χ_i represents the exact solution at x_i, whereas $\tilde{\chi}$ represents the numerical solution at x_i. L_∞ is the standard maximum absolute error norm. L_∞ also represents the conventional maximum absolute error norm.

5.1. Example 1

Consider $\mu = -1$ for this example, in which case the MEW in Eq (1.1) becomes

$$\chi_t + 3\chi^2\chi_x + \chi_{xxt} = 0, \tag{5.4}$$

over $x \in [-10, 10]$ and $t \in [0, 1]$ with the following initial and boundary conditions:

$$\chi(x, 0) = 0.7 \tanh(0.7x), \tag{5.5}$$

$$\chi(-10, t) = -0.7, \tag{5.6}$$

$$\chi(10, t) = 0.7. \tag{5.7}$$

The numerical solution $\tilde{\chi}_1(x, t)$ is demonstrated in Figure 5, along with the analytical solution $\chi_1(x, t)$, which was previously derived and is shown in Eq (3.15), using $h = 0.01$ and $\delta t = 0.001$. We also use the L_2-norm and the L_∞-norm to compare the numerical errors, as presented in Table 1. Therefore, the numerical results are accurate up to 10^{-5} according to the Euclidean norm.

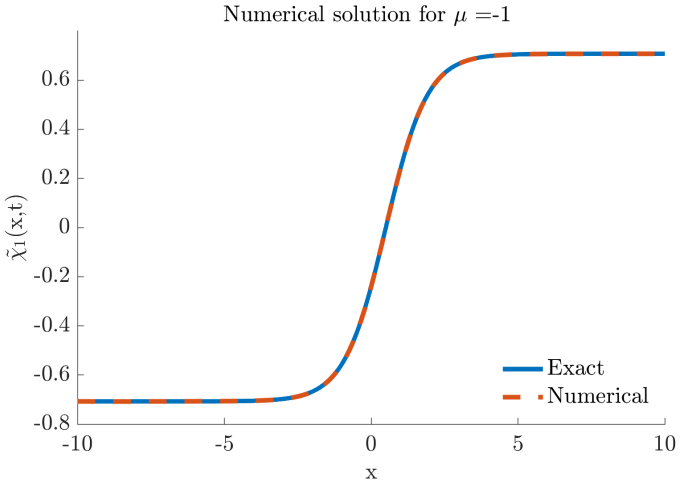

Figure 5. A comparison of the analytical solution $\chi_1(x, t)$ given in (3.15) with the numerically computed solution $\tilde{\chi}_1(x, t)$ of (5.4), evaluated across the spatial domain $x \in [-10, 10]$ at $t = 1$, using the discretisation parameters $h = 0.01$ (spatial) and $\delta t = 0.001$ (temporal).

Table 1. An illustration of the numerical results compared with the analytical solution given in Eq (3.15) using the L_2-norm and L_∞-norm.

	Example 1	Example 2	Example 3	Example 4
μ	-1	-0.9	-1.5	-0.16
v	0.5	0.1	0.75	1.00E-03
L_∞	5.86E-04	8.91E-07	1.40E-03	3.06E-10
L_2	8.44E-05	1.98E-07	2.58E-04	2.75E-11
h	0.01			0.001
x	[-10, 10]			
δt	0.001			

5.2. *Example 2*

For this example, let $\mu = -0.9$. The MEW Eq (1.1) then becomes

$$\chi_t + 3\chi^2\chi_x + 0.9\chi_{xxt} = 0, \tag{5.8}$$

over $x \in [-10, 10]$ and $t \in [0, 1]$ with the following initial and boundary conditions:

$$\chi(x, 0) = \frac{1}{3} \tanh(\frac{1}{4}x), \tag{5.9}$$

$$\chi(-10, t) = -\frac{1}{3}, \tag{5.10}$$

$$\chi(10, t) = \frac{1}{3}. \tag{5.11}$$

The analytical solution $\chi_1(x, t)$ given in Eq (3.15) is shown alongside the numerical solution $\tilde{\chi_1}(x, t)$ in Figure 6 with $h = 0.01$, $\delta t = 0.001$, and we compared the numerical errors in Table 1 using the L_2-norm and L_∞-norm. Hence, using the Euclidean norm, the numerical results are accurate to 10^{-7}.

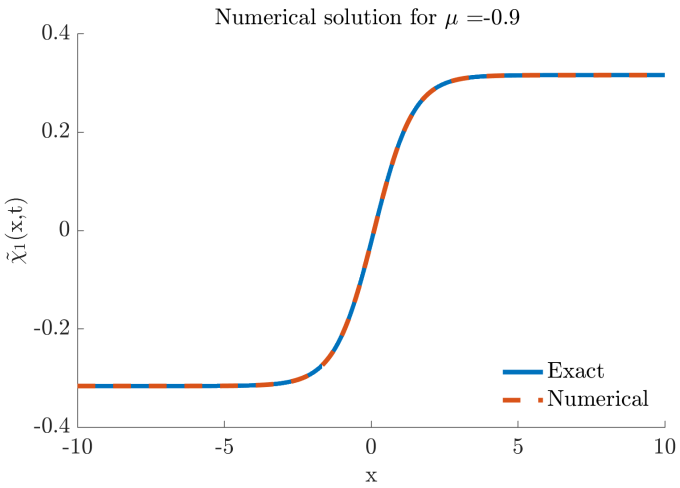

Figure 6. A comparison of the analytical solution $\chi_1(x, t)$ given in (3.15) with the numerically computed solution $\tilde{\chi_1}(x, t)$ of (5.8), evaluated across the spatial domain $x \in [-10, 10]$ at $t = 1$, using the discretisation parameters $h = 0.01$ (spatial) and $\Delta t = 0.001$ (temporal).

For Examples 3 and 4, where $\mu = \{-1.5, -0.16\}$, we present only the numerical errors of these examples in Table 1, alongside the results of Examples 1 and 2, to demonstrate the effect of μ. As the value of μ was altered, we observed that the numerical method produced accurate results up to 10^{-11} according to the Euclidean norm as μ decreased.

5.3. Example 5

For this example, let $\mu = -0.9$. The in MEW Eq (1.1) then becomes

$$\chi_t + 3\chi^2\chi_x + 0.9\chi_{xxt} = 0, \tag{5.12}$$

over $x \in [0.1, 4]$ and $t \in [0, 1]$ with the following initial and boundary conditions:

$$\chi(x, 0) = 0.031 \coth(\frac{3}{4}x), \tag{5.13}$$

$$\chi(0.1, t) = 0.42, \tag{5.14}$$

$$\chi(4, t) = 0.031. \tag{5.15}$$

If we use the spatial and temporal steps $h = 0.01$ and $\Delta t = 0.001$, respectively, the analytical solution $\chi_3(x, t)$ previously derived and shown in (3.16) and its numerical approximation $\tilde{\chi}_3(x, t)$ are shown in Figure 7. The Euclidean norm measurement of the numerical solution yields an accuracy of $O(10^{-4})$.

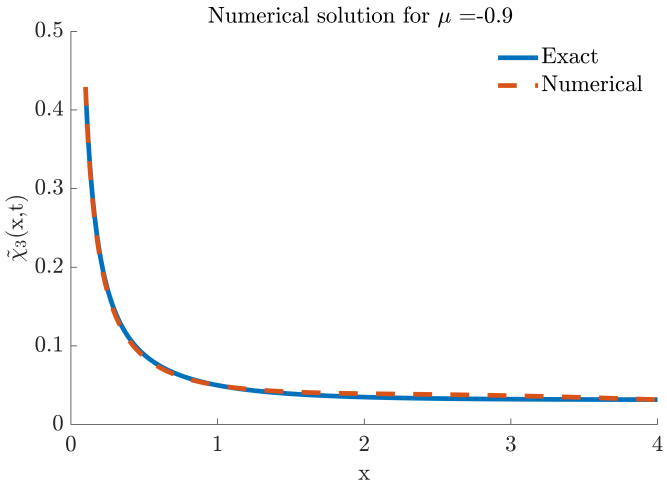

Figure 7. A comparison of the analytical solution $\chi_3(x, t)$ given in (3.16) with the numerically computed solution $\tilde{\chi}_3(x, t)$ of (5.12), evaluated across the spatial domain $x \in [0.1, 4]$ at $t = 1$, using the discretisation parameters $h = 0.01$ (spatial) and $\Delta t = 0.001$ (temporal).

6. Conclusions

A closed-form method for examining nonlinear wave phenomena is the MEW model, especially in systems where dispersion and nonlinearity are both crucial. It is a useful model in fluid dynamics, optics, and plasma physics because of its capacity to generate soliton solutions and simulate a variety of physical systems. The MEW equation is a testbed for developing and improving analytical and numerical approaches in nonlinear wave theory. We applied the closed-form technique and introduced the solitary wave solutions to the MEW equation. Namely, we introduced different families of solitary wave solutions through physical parameters. For suitable free parameter values, some 2D and 3D charts are supplied to show the dynamic behavior of the solutions that are presented. Additionally, we employed a creative finite difference technique to demonstrate the MEW model's numerical solution. The accuracy of the procedure is shown by a comparison with the analytical solution we arrived at. This study demonstrates that changes in time stepping, wave speed, and spatial discretisation do not affect the numerical method's stability and accuracy. On the basis of this analytical and numerical research, the MEW model's solutions are predicted to exhibit localized, stable, and coherent structures such as solitons, kinks, or compactons, depending on the parameter regime and initial conditions. It is expected that these waveforms will maintain their amplitude, shape, and velocity over time, even following interactions, thereby demonstrating the model's ability to uphold the integrity of nonlinear waves.

Use of Generative-AI tools declaration

The author declare that he has not used artificial intelligence (AI) tools in the creation of this article.

Conflict of interest

The authors declare that they have no competing interests.

References

1. S. J. Chen, X. Lü, M. G. Li, F. Wang, Derivation and simulation of the M-lump solutions to two (2+1)-dimensional nonlinear equations, *Phys. Scripta*, **96** (2021), 095201. https://doi.org/10.1088/1402-4896/abf307
2. Y. Kai, Z. Yin, On the Gaussian traveling wave solution to a special kind of Schrödinger equation with logarithmic nonlinearity, *Mod. Phys. Lett. B*, **02** (2022), 2150543. https://doi.org/10.1142/S0217984921505436
3. M. Shakeel, Attaullah, N. A. Shah, J. D. Chung, Application of modified exp-function method for strain wave equation for finding analytical solutions, *Ain Shams Eng. J.*, **14** (2023), 101883. https://doi.org/10.1016/j.asej.2022.101883
4. H. Triki, C. Bensalem, A. Biswas, S. Khan, Q. Zhou, S. Adesanya, et al., Self-similar optical solitons with continuous-wave background in a quadratic-cubic non-centrosymmetric waveguide, *Opt. Commun.*, **437** (2019), 392–398. https://doi.org/10.1016/j.optcom.2018.12.074
5. L. Q. Kong, C. Q. Dai, Some discussions about variable separation of nonlinear models using Riccati equation expansion method, *Nonlinear Dynam.*, **81** (2015), 1553–1561. https://doi.org/10.1007/s11071-015-2089-y
6. Y. Y. Wang, Y. P. Zhang, C. Q. Dai, Re-study on localized structures based on variable separation solutions from the modified tanh-function method, *Nonlinear Dynam.*, **83** (2016), 1331–1339. https://doi.org/10.1007/s11071-015-2406-5
7. A. H. Arnous, M. S. Hashemi, K. S. Nisar, M. Shakeel, J. Ahmad, I. Ahmad, et al., Investigating solitary wave solutions with enhanced algebraic method for new extended Sakovich equations in fluid dynamics, *Results Phys.*, **57** (2024), 107369. https://doi.org/10.1016/j.rinp.2024.107369
8. Y. Zhu, J. Yang, Y. Zhang, W. Qin, S. Wang , J. Li, Ring-like double-breathers in the partially nonlocal medium with different diffraction characteristics in both directions under the external potential, *Chaos Soliton. Fract.*, **180** (2024), 114510. https://doi.org/10.1016/j.chaos.2024.114510
9. G. Arora, R. Rani, H. Emadifar, Soliton: A dispersion-less solution with existence and its types, *Heliyon*, **8** (2022), e12122. https://doi.org/10.1016/j.heliyon.2022.e12122
10. Z. Z. Si, Y. Y. Wang, C. Q. Dai, Switching, explosion, and chaos of multi-wavelength soliton states in ultrafast fiber lasers, *Sci. China Phys. Mech.*, **67** (2024), 274211. https://doi.org/10.1007/s11433-023-2365-7
11. M. G. Hafez, M. N. Alam, M. A. Akbar, Exact traveling wave solutions to the Klein-Gordon equation using the novel (G'/G)-expansion method, *Results Phys.*, **4** (2014), 177–184. https://doi.org/10.1016/j.rinp.2014.09.001

12. H. U. Rehman, I. Iqbal, S. S. Aiadi, N. Mlaiki, M. S. Saleem, Soliton solutions of Klein-Fock-Gordon equation using Sardar subequation method, *Mathematics*, **10** (2022), 3377. https://doi.org/10.3390/math10183377

13. A. Alsisi, Analytical and numerical solutions to the Klein-Gordon model with cubic nonlinearity, *Alex. Eng. J.*, **99** (2024), 31–37. https://doi.org/10.1016/j.aej.2024.04.076

14. M. S. Attaullah, E. R. E. Zahar, N. A. Shah, J. D. Chung, Generalized exp-function method to find closed form solutions of nonlinear dispersive modified Benjamin-Bona-Mahony equation defined by seismic sea waves, *Mathematics*, **10** (2022), 1026. https://doi.org/10.3390/math10071026

15. D. Marek, D. Lucjan, Nonlinear Klein-Gordon equation in Cauchy-Navier elastic solid, *Cherkasy U. B. Phys. Math. Sci.*, **1** (2017), 22–29.

16. S. I. Zaki, Solitary wave interactions for the modified equal width equation, *Comput. Phys. Commun.*, **126** (2000), 219–231. https://doi.org/10.1016/S0010-4655(99)00471-3

17. D. H. Peregrine, Calculations of the development of an undular bore, *J. Fluid Mech.*, **25** (1966), 321–330. https://doi.org/10.1017/S0022112066001678

18. A. K. M. K. S. Hossain, M. A. Akbar, A. M. Wazwaz, Closed form solutions of complex wave equations via MSE method, *Cogent Phys.*, **4** (2017), 1312751. https://doi.org/10.1080/23311940.2017.1312751

19. B. Saka, Algorithms for numerical solution of the modified equal width wave equation using collocation method, *Math. Comput. Model.*, **45** (2007), 1096–1117. https://doi.org/10.1016/j.mcm.2006.09.012

20. A. M. Wazwaz, The tanh and the sine-cosine methods for a reliable treatment of the modified equal width equation and its variants, *Commun. Nonlinear Sci.*, **11** (2006), 148–160. https://doi.org/10.1016/j.cnsns.2004.07.001

21. B. Saka, I. Dağ, Quartic B-spline collocation method to the numerical solutions of the Burgers' equation, *Chaos Soliton. Fract.*, **32** (2007), 1125–1137. https://doi.org/10.1016/j.chaos.2005.11.037

22. A. Başhan, N. M. Yağmurlu, Y. Uçar, A. Esen, A new perspective for the numerical solution of the modified equal width wave equation, *Math. Method. Appl. Sci.*, **44** (2021), 8925–8939. https://doi.org/10.1002/mma.7322

23. N. M. Yağmurlu, A. S. Karakaş, A novel perspective for simulations of the MEW equation by trigonometric cubic B-spline collocation method based on Rubin-Graves type linearization, *Comput. Methods Diffe.*, **10** (2022), 1046–1058. https://doi.org/10.22034/cmde.2021.47358.1981

24. G. Fan, B. Wu, Numerical solutions of the EW and MEW equations using a fourth-order improvised B-spline collocation method, *Numerical Algorithms*, **98** (2025), 1799–1825. https://doi.org/10.1007/s11075-024-01853-5

25. E. Kirli, S. Cikit, A high order accurate hybrid technique for numerical solution of modified equal width equation, *Wave Motion*, **135** (2025), 103508. https://doi.org/10.1016/j.wavemoti.2025.103508

26. I. Onder, M. Cinar, A. Secer, M. Bayram, On soliton solutions of the modified equal width equation, *Eng. Computation.*, **40** (2023), 1063–1083. https://doi.org/10.1108/EC-08-2022-0529

27. A. M. Wazwaz, The extended tanh method for new solitons solutions for many forms of the fifth-order KdV equations, *Appl. Math. Comput.*, **184** (2007), 1002–1014. https://doi.org/10.1016/j.amc.2006.07.002

28. X. Wang, J. Wu, Y. Wang, C. Chen, Extended tanh-function method and its applications in nonlocal complex mKdV equations, *Mathematics*, **10** (2022), 3250. https://doi.org/10.3390/math10183250

29. A. Esen, S. Kutluay, Solitary wave solutions of the modified equal width wave equation, *Commun. Nonlinear Sci.*, **13** (2008), 1538–1546. https://doi.org/10.1016/j.cnsns.2006.09.018

AIMS Press